An efficient hybrid transfer matrix-statistical energy analysis approach for predicting the sound transmission through thick and layered walls

Edwin Reynders, Arne Dijckmans and Carolina Decraene

KU Leuven, Department of Civil Engineering

Kasteelpark Arenberg 40, B-3001 Leuven, Belgium

Abstract

In this work, an efficient method is developed for computing the diffuse sound transmission of walls and floors that consist of layers of solid, fluid and/or poroelastic material. This is achieved by coupling a transfer matrix model of the wall or floor to statistical energy analysis subsystem models of the adjacent room volumes, which obviates the need for numerically integrating the plane wave transmission coefficient for all possible angles of incidence. The modal behavior of the wall is approximately accounted for by projecting the wall displacement onto a set of sinusoidal lateral basis functions. The method is applied for predicting the airborne sound insulation of a thin plate, a thick wall and a sandwich panel. The predictions are compared with alternative predictions and with measured values. A good overall agreement is observed.

1 Introduction

Layered wall and floor systems are very frequently applied in order to achieve a high thermal and/or sound insulation with a relatively low weight. Examples are double walls with decoupled wall leafs, roof panels, floors with floating screeds, double and triple glazing, etc. At high frequencies, the airborne or impact sound transmission through such layered systems can be computed with high accuracy using the transfer matrix method (TMM) [1, 2]. It is then assumed that the wall or floor is of infinite lateral extent. This enables modeling the sound transmission through each solid, fluid and/or poro-elastic layer analytically in the frequency-wavenumber domain.

However, the conventional TMM has two disadvantages. Firstly, the assumption of an infinite wall may lead to important prediction errors at lower frequencies. The influence of diffraction effects may be accounted for by spatial windowing [3], but in this way the modal behavior of the wall is still neglected. An alternative has therefore been developed [4, 5], in which the wall displacement is projected onto a set of sinusoidal lateral basis functions, such that the wall impedance at a given frequency and for a given lateral basis function (hence lateral wavenumber) can be computed using the TMM. This approach approach accounts approximately for modal wall behavior when the boundary conditions are simply supported.

A second disadvantage is that the computation of the mean diffuse-field transmission involves numerical integration of the plane-wave transmission over all possible angles of incidence. This is computationally expensive, especially when it needs to be combined with spatial windowing or the approximate modal technique. Furthermore, the variance of the transmission loss which is caused by the diffuse field assumption cannot be computed.

Therefore, an alternative approach is developed here, in which the diffuse fields in the rooms are modeled as in statistical energy analysis (SEA), while the wall is still modeled deterministically, using the TMM with the approximate modal technique. This hybrid TMM-SEA approach accounts for the finite dimensions and approximately for the modal behavior of the wall while it is computationally very efficient, since the diffuse sound fields in the rooms are modeled as SEA subsystems, which obviates the need to numerically integrate the plane wave transmission

over all angles of incidence. The hybrid TMM-SEA approach can be considered as an extension of the hybrid finite element - statistical energy analysis (FE-SEA) approach to vibro-acoustic analysis [6, 7, 8, 9], where the FE model of a layered wall is replaced by a more efficient TMM model.

The remainder of this article is organized as follows. Section 2 introduces the hybrid deterministic-SEA approach to sound transmission modeling in general, while section 3 makes the connection with the transfer matrix method. Subsequently, the performance of this hybrid TMM-SEA approach is investigated in detail for three walls, by comparing the predicted sound insulation values with other predictions and with measured values. The considered wall types are a thin plate (section 4), a thick wall (section 5) and a sandwich panel (section 6). The conclusions are presented in section 7.

2 Hybrid deterministic-SEA sound transmission modelling

Throughout this article, a room-wall-room system is considered, where the rooms carry a diffuse field but the wall does not. The out-of-plane displacement u_z of the partition wall is decomposed using a set of N_m global basis functions ϕ (which are usually the in-vacuo modes) and corresponding generalized coordinates q. For example, when the wall is modeled as a plate or shell, one has

$$u_\mathrm{z}(x,y,\omega) \approx \sum_{p=1}^{N_\mathrm{m}} \phi_p(x,y) q_p(\omega) \tag{1}$$

When a volumetric model of the wall is employed, the decomposition is made for each of both outer surfaces A and B:

$$u_\mathrm{z}(x,y,z_\mathrm{A},\omega) \approx \sum_{p=1}^{N_\mathrm{m}} \phi_p(x,y,z_\mathrm{A}) q_{p\mathrm{A}}(\omega) \qquad \text{and} \qquad u_\mathrm{z}(x,y,z_\mathrm{B},\omega) \approx \sum_{p=1}^{N_\mathrm{m}} \phi_p(x,y,z_\mathrm{B}) q_{p\mathrm{B}}(\omega) \tag{2}$$

Let us collect all generalized response degrees of freedom (DOFs) in an amplitude vector $\mathbf{q}(\omega) \in \mathbb{C}^{N_\mathrm{dof}}$, so that the time-domain response is given by $\mathrm{Re}(\mathbf{q}\mathrm{e}^{i\omega t})$. Similarly, the corresponding generalized harmonic loads are collected in the load amplitude vector $\mathbf{f}(\omega) \in \mathbb{C}^{N_\mathrm{dof}}$. Note that, when the wall is modeled as a plate or shell, $N_\mathrm{dof} = N_\mathrm{m}$, but when it is modeled as a volume, $N_\mathrm{dof} = 2N_\mathrm{m}$. Since $\mathbf{q}$ contains all (generalized) interface degrees of freedom between the wall and the rooms, the equations of motion of the whole system (room-wall-room) can be written as

$$\mathbf{D}\mathbf{q} = \mathbf{f}, \tag{3}$$

with $\mathbf{D} \in \mathbb{C}^{N_\mathrm{dof} \times N_\mathrm{dof}}$ the dynamic stiffness matrix at frequency ω. $\mathbf{D}$ may be decomposed as the sum of the dynamic stiffness matrix of the wall, denoted as $\mathbf{D}_\mathrm{d}$ (subscript d stands for deterministic), and the dynamic stiffness matrices of the rooms, which are both random subsystems, denoted as $\mathbf{D}_1$ and $\mathbf{D}_2$:

$$\mathbf{D} = \mathbf{D}_\mathrm{d} + \mathbf{D}_1 + \mathbf{D}_2 \tag{4}$$

The dynamic stiffness matrix of a random subsystem (acoustic room volume) is decomposed as

$$\mathbf{D}_k = \mathbf{D}_\mathrm{dir}^{(k)} + \mathbf{D}_\mathrm{rev}^{(k)}, \tag{5}$$

where $\mathbf{D}_\mathrm{dir}^{(k)} := \mathrm{E}\left[\mathbf{D}_k\right]$. With this decomposition, the equations of motion for a random subsystem are

$$\mathbf{D}_\mathrm{dir}^{(k)}\mathbf{q} = \mathbf{f}_k + \mathbf{f}_\mathrm{rev}^{(k)}, \tag{6}$$

where the reverberant forces are defined as $\mathbf{f}_\mathrm{rev}^{(k)} := -\mathbf{D}_\mathrm{rev}^{(k)}\mathbf{q}$, and $\mathbf{f}_k$ denotes the sum of the loads applied to subsystem k at its DOFs. The overall equations of motion (3) become

$$\mathbf{D}_\mathrm{tot}\mathbf{q} = \mathbf{f} + \mathbf{f}_\mathrm{rev}^{(1)} + \mathbf{f}_\mathrm{rev}^{(2)}, \tag{7}$$

where $\mathbf{D}_\mathrm{tot} := \mathbf{D}_\mathrm{d} + \sum_{k=1}^{2} \mathbf{D}_\mathrm{dir}^{(k)}$ is a purely deterministic matrix.

When a diffuse field acts in both rooms and these fields are statistically independent of each other, the mean time-averaged total energy $\hat{E}_j$ of room j can be obtained from a stationary power balance which involves the other random subsystems as well as the deterministic master system. For the case where the external loading acts solely on the random subsystems (rooms), this reads [6]:

$$\omega\left(\eta_j + \eta_{\mathrm{d},j}\right)\hat{E}_j + \sum_{k=1}^{2} \omega\eta_{jk} n_j \left(\frac{\hat{E}_j}{n_j} - \frac{\hat{E}_k}{n_k}\right) = \mathrm{E}[P_j], \qquad j = 1,2. \tag{8}$$

In this expression, η_j is the damping loss factor of subsystem j, n_j its modal density, P_j the power input from external forces applied directly to this subsystem, and

$$\omega\eta_{\mathrm{d},j} = \frac{2}{\pi n_j} \sum_{r,s} \mathrm{Im}\left(D_{\mathrm{d},rs}\right) \left(\mathbf{D}_{\mathrm{tot}}^{-1} \mathrm{Im}\left(\mathbf{D}_{\mathrm{dir}}^{(j)}\right) \mathbf{D}_{\mathrm{tot}}^{-\mathrm{H}}\right)_{rs} \tag{9}$$

$$\omega\eta_{jk} n_j = \frac{2}{\pi} \sum_{r,s} \mathrm{Im}\left(D_{\mathrm{dir},rs}^{(j)}\right) \left(\mathbf{D}_{\mathrm{tot}}^{-1} \mathrm{Im}\left(\mathbf{D}_{\mathrm{dir}}^{(k)}\right) \mathbf{D}_{\mathrm{tot}}^{-\mathrm{H}}\right)_{rs} \tag{10}$$

where the superscript H denotes Hermitian transpose. If the wall provides sufficient sound insulation, $\mathrm{E}[P_j]$ can be approximated as the mean power input to the decoupled room. It can be noted that the power balance equation (8) has formally the same structure as in standard SEA. Therefore the factors η_{jk} can be interpreted as coupling loss factors, and (10) provides a rigorous way to compute them, even when the overall system is partly deterministic.

The mean sound reduction index can be computed by solving the system of two equations (8) in two unknowns ($\hat{E}_1$ and $\hat{E}_2$) for a given excitation in the sending room, e.g., $P_1 = 1$ and $P_2 = 0$. Once this has been performed, the mean sound reduction index follows from [9]

$$\mathrm{E}[R] \approx 10 \log \frac{\hat{E}_1 V_2 S}{\hat{E}_2 V_1 A_2}, \tag{11}$$

where S is the surface area of the partition wall, and A_2 the acoustic absorption in the receiving room, and V_1 and V_2 the volumes of the sending and receiving room, respectively.

Before the system of equations (8) can be solved however, some subsystem-related quantities are needed. The damping loss factors of the rooms can be obtained from the corresponding reverberation times via

$$\eta = \frac{4.4\pi}{\omega T} \tag{12}$$

The modal density of a room can be estimated as [10]

$$n(\omega) = \frac{\omega^2 V}{2\pi^2 c^3} \tag{13}$$

where c denotes the sound speed.

The frequency-dependent matrix $\mathbf{D}_{\mathrm{dir}}^{(k)}$ can be computed as the direct field receptance matrix of room (subsystem) k [11, 12]. The term 'direct field' denotes the part of the subsystem response containing outgoing waves only; it is the limiting response that would be observed at the interface when the extent of the subsystem would be increased. For the case of a transmission suite, where two rooms are separated by a plane flexible structure of finite size, the direct field dynamic stiffness matrix of a room as seen by the structure corresponds to the one of a grid of points covering the interface between the room and the structure, but embedded in an infinite planar baffle facing an acoustic halfspace. In order to evaluate this stiffness matrix, the wavelet approach [13] is followed in this article. The obtained force-displacement dynamic stiffness matrix is then projected onto the generalized coordinates.

Finally, the dynamic stiffness matrix of the wall $\mathbf{D}_{\mathrm{d}}$ in modal coordinates is needed. When the wall is a thin simply supported plate of dimensions $L_x \times L_y \times t$, a natural choice for the basis functions in (1) are the exact plate mode shapes, which are [10, Sec. 5.7.2]

$$\phi_p(x,y) = \sin\left(\frac{p_x \pi x}{L_x}\right) \sin\left(\frac{p_y \pi y}{L_y}\right), \tag{14}$$

where p_x and p_y denote the integer number of half wavelengths in the x and y directions, respectively, of mode p. The elements of the dynamic stiffness matrix are then

$$D_{\mathrm{d},pq}(\omega) = \frac{\rho t L_x L_y}{4} \left(-\omega^2 + \omega_p^2(1+\eta_{\mathrm{p}})\right) \delta_{pq} \tag{15}$$

where ρ denotes the density of the plate material, δ_{pq} the Kronecker delta, η_{p} the loss factor of the plate, and ω_p the natural frequency of mode p:

$$\omega_p = \sqrt{\frac{D}{\rho t}} \left(k_{px}^2 + k_{py}^2\right), \qquad D := \frac{E t^3}{12(1-\nu^2)}, \quad k_{px} := \frac{p_x \pi}{L_x}, \quad k_{py} := \frac{p_y \pi}{L_y} \tag{16}$$

with E the Young's modulus of the plate and ν the Poisson's ratio.

For thick or multilayered walls, the dynamic stiffness matrix D_{d} will need to be computed in a different way, e.g., by means of a finite element model [6, 7, 9]. In the next section, a more efficient approach is presented, which makes the link with the transfer matrix method.

3 Computing finite wall impedances with the transfer matrix method

The transfer matrix method [1, 2] is an efficient framework that allows computing the mechanical impedance matrix $\mathbf{Z}(k_x, \omega)$ for two-dimensional (x-z) wave propagation between both sides of an infinite wall consisting of solid, fluid and/or poroelastic layers for a given longitudinal wavenumber k_x and a given frequency ω:

$$\begin{bmatrix} Z_{11}(k_x,\omega) & Z_{12}(k_x,\omega) \\ Z_{21}(k_x,\omega) & Z_{22}(k_x,\omega) \end{bmatrix} \begin{bmatrix} v_{\mathrm{zA}}(k_x,\omega) \\ v_{\mathrm{zB}}(k_x,\omega) \end{bmatrix} = \begin{bmatrix} p_{\mathrm{A}}(k_x,\omega) \\ p_{\mathrm{B}}(k_x,\omega) \end{bmatrix} \tag{17}$$

where v_{zA} and v_{zB} denote the velocities and p_{A} and p_{B} the pressures at sides A and B of the wall, respectively.

For finite walls with simply supported boundaries, the out-of-plane displacement $u_{\mathrm{z}}(x, y, z, \omega)$ can be approximated as

$$u_{\mathrm{z}}(x, y, z, \omega) \approx \sum_{p=1}^{N_{\mathrm{m}}} \phi_p(x, y) q_p(z, \omega), \tag{18}$$

The plate velocities and the pressures at both wall sides can then be written as [4, 5]

$$\begin{bmatrix} v_{\mathrm{zA}}(x,y,\omega) \\ v_{\mathrm{zB}}(x,y,\omega) \end{bmatrix} = \sum_p \begin{bmatrix} V_{\mathrm{zAp}}(\omega) \\ V_{\mathrm{zBp}}(\omega) \end{bmatrix} \phi_p(x,y) \qquad \text{and} \qquad \begin{bmatrix} p_{\mathrm{A}}(x,y,\omega) \\ p_{\mathrm{B}}(x,y,\omega) \end{bmatrix} = \sum_p \begin{bmatrix} P_{\mathrm{Ap}}(\omega) \\ P_{\mathrm{Bp}}(\omega) \end{bmatrix} \phi_p(x,y) \tag{19}$$

When $\phi_p(x, y)$ is chosen as in (14), it corresponds to a bending mode shape of a finite, homogenous thin plate, with modal wavenumber

$$k_p = \sqrt{k_{px}^2 + k_{py}^2} \tag{20}$$

The modal response of this homogenous thin plate can also be obtained by imposing this modal wavenumber as trace wavenumber in an infinite plate model. Since the basis functions $\phi_p(x, y)$ are also orthogonal to each other, one has the following exact relationship for a finite homogenous thin plate:

$$\begin{bmatrix} Z_{11}(k_p,\omega) & Z_{12}(k_p,\omega) \\ Z_{21}(k_p,\omega) & Z_{22}(k_p,\omega) \end{bmatrix} \begin{bmatrix} V_{\mathrm{zAp}}(\omega) \\ V_{\mathrm{zBp}}(\omega) \end{bmatrix} = \begin{bmatrix} P_{\mathrm{Ap}}(\omega) \\ P_{\mathrm{Bp}}(\omega) \end{bmatrix} \tag{21}$$

This implies that (1) the impedances of the wall in the chosen generalized coordinates can be computed independently for each basis function, and (2) the impedance matrix between both sides of a finite wall in generalized coordinates can be evaluated as the impedance matrix of the corresponding infinite wall, evaluated for the wavenumber k_p of the basis function p. The dynamic stiffness matrix of the plate in generalized coordinates then follows from

$$\mathbf{D}_{\mathrm{d,p}}(\omega) = \frac{i\omega L_x L_y}{4} \mathbf{Z}(k_p, \omega) \tag{22}$$

where the factor $i\omega$ originates from the transformation from modal velocity to modal displacement, and the factor $\frac{L_x L_y}{4}$ originates from the transformation from modal pressure to modal force:

$$f_p = \int_0^{L_x} \int_0^{L_y} p(x,y)\phi_p(x,y)dxdy = \int_0^{L_x} \int_0^{L_y} P_p \phi_p^2(x,y)dxdy = P_p \frac{L_x L_y}{4} \tag{23}$$

Eq. (22) is only exact for thin simply supported thin plate. Its validity for other wall types depends on the validity of the approximation (18), which assumes that only waves with modal wavenumbers k_p can propagate through the structure.

4 Application 1: thin PMMA plate

As a first application, the sound transmission loss of a thin, simply supported polymethyl mathacrylate (PMMA) panel is computed with the hybrid TMM-SEA approach outlined above. The aim here is to validate the evaluation of the dynamic stiffness matrix of the wall via the TMM vs. a direct, analytical evaluation via (15). The PMMA panel has a density $\rho = 1275\,\frac{\mathrm{kg}}{\mathrm{m}^3}$, modulus of Elasticity $E = 4.5\,\mathrm{GPa}$, Poisson's ratio $\nu = 0.35$ and dimensions $1.25\,\mathrm{m} \times 1.50\,\mathrm{m} \times 0.015\,\mathrm{m}$. For the damping ratio, measured values are used (see [9, Table 1]). The adjacent acoustic spaces have a volume $87\,\mathrm{m}^3$, reverberation time $T = 1.5\,\mathrm{s}$, air density $1.2\,\frac{\mathrm{kg}}{\mathrm{m}^3}$ and sound speed of $343\,\frac{\mathrm{m}}{\mathrm{s}}$.

Fig. 1 compares the analytic and the TMM-based hybrid predictions with each other. There is an excellent agreement below $1000\,\mathrm{Hz}$, which confirms that both approaches are equivalent for thin, simply supported plates. The differences near the coincidence dip, which is situated around $2500\,\mathrm{Hz}$, are probably due to shear deformation and rotational inertia, which are not included in the analytic hybrid predictions, but they are in the TMM-based hybrid predictions. The hybrid TMM-SEA results are also compared against narrow-band (1/48 octave) transmission

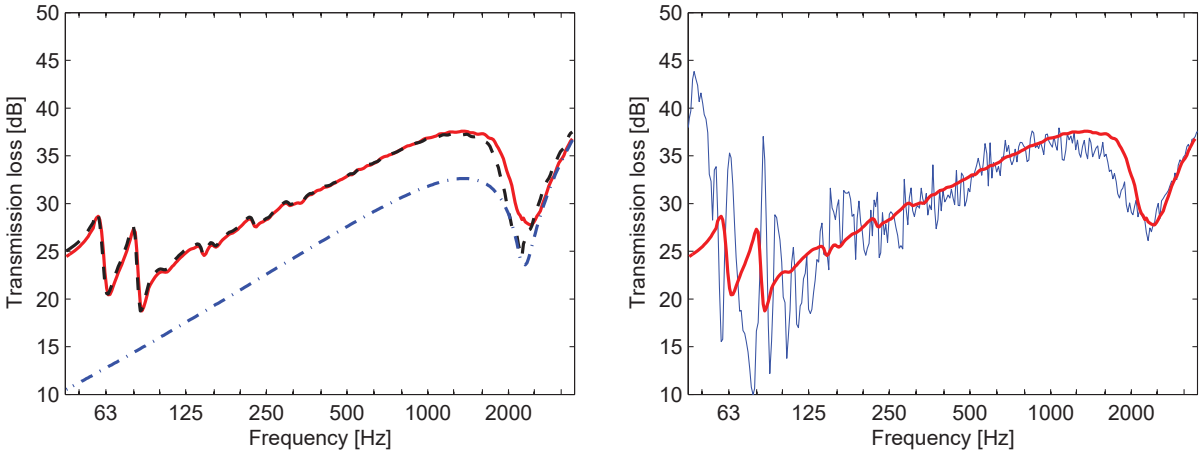

Figure 1: Sound transmission loss of a PMMA panel as predicted with the hybrid TMM-SEA approach (red solid line), as predicted with the hybrid analytical-SEA approach (black dashed line), as predicted with conventional TMM (blue dash-dotted line) and as measured in the laboratory (thin blue line)

loss measurements that have been performed at the KU Leuven Acoustics Laboratory [9, 14]. Below the Schroeder frequency [15] of the rooms, which is at 263 Hz, there is a strong oscillation in the measured sound transmission loss, since individual room modes influence the transmission loss. Above the Schroeder frequency, the measured transmission loss values are close to the predicted values, which are the mean values for diffuse sound fields in the rooms. Finally, the predictions are also compared against conventional TMM predictions, which do not account for the finite dimensions and the modal behavior of the plate. A conventional TMM model clearly underestimate the sound transmission loss of the plate below coincidence. Above coincidence, the conventional TMM predictions coincide with the hybrid TMM-SEA predictions, which indicates that at this high frequencies, neither the finite dimensions nor the modal behavior of the plate influence the sound transmission loss.

5 Application 2: hollow brick wall

The second wall that is considered is a perforated brick wall of dimensions $3.25\,\mathrm{m} \times 2.95\,\mathrm{m} \times 0.19\,\mathrm{m}$, plastered at both sides. The acoustic behavior of perforated brick walls is complex, given the inhomogeneities at three different scales: the fire clay material, the brick where small cavities are present in the fire clay because of the perforations, and the entire wall where the bricks are held together by mortar layers. When the inhomogeneities

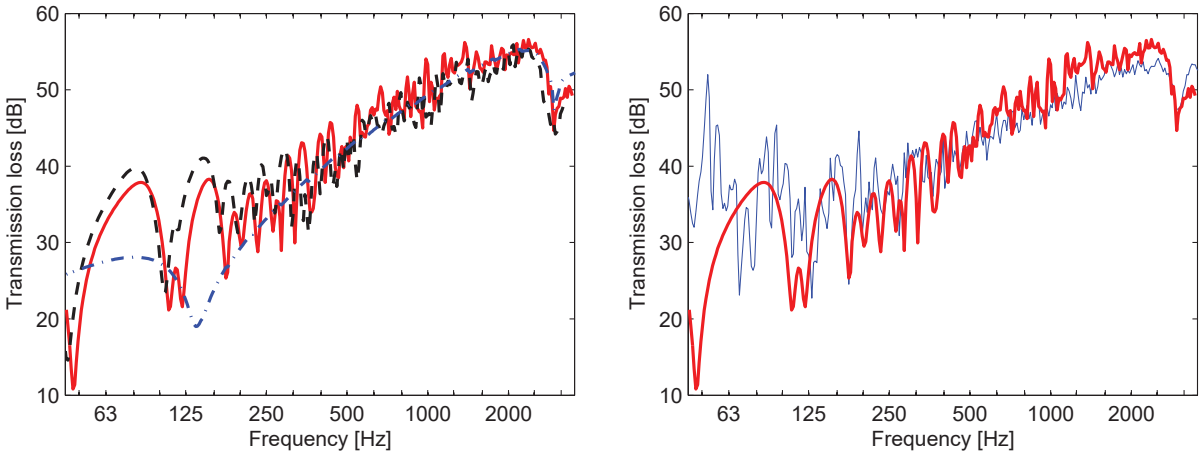

Figure 2: Sound transmission loss of a perforated brick wall as predicted with the hybrid TMM-SEA approach (red solid line), as predicted with the hybrid analytical-SEA approach (black dashed line), as predicted with conventional TMM (blue dash-dotted line), and as measured in the laboratory (thin blue line)

are small compared to the wavelength, and when the stiffness is only slightly different in both directions, the wall can be modeled as homogeneous and isotropic. The thickness effects, however, can not be neglected: not only is shear deformation important, thickness resonances (i.e., Lamb modes) are often observed in the audio frequency range [16]. Following [4], the equivalent Young's modulus, Poisson's ratio, density and thickness of the considered wall are taken as $E = 1825$ MPa, $\nu = 0.2$, $\rho = 613.5\ \frac{\text{kg}}{\text{m}^3}$ and $t = 0.2934$ m, respectively. For the damping ratio, measured values are used (see Table [9, Table 1]). The rooms are the same as before.

Fig. 2 compares the hybrid TMM-SEA predictions with conventional TMM predictions and with predictions using a hybrid FE-SEA model that have been reported earlier [9]. In the hybrid FE-SEA model, the wall is modeled using 8-node solid linear elastic finite elements (of the SOLID45 element type in ANSYS) and only the boundary displacements in the middle plane of the wall are restrained. The hybrid TMM-SEA and FE-SEA predictions agree well but they are not exactly the same, which is expected since the boundary conditions are slightly different and since (18) results in an approximation of the true wall behavior for thick walls. Both models correctly predict the first thickness resonance of the wall at around 3000 Hz. The comparison with the conventional TMM predictions illustrate that the modal behavior of the wall plays an important role up to about 500 Hz. The low modal density of the wall makes that the coincidence dip, which can be observed in the conventional TMM predictions between 125 Hz and 160 Hz, cannot develop. This is confirmed by the comparison of the hybrid TMM-SEA results with measured values [9]; again a good agreement is observed above the Schroeder frequency of the rooms, where the modal behavior of these rooms plays a less important role.

6 Application 3: sandwich panel

The final application concerns a sandwich panel of dimensions $1.25\,\text{m} \times 1.50\,\text{m} \times 0.150\,\text{m}$. The panel consists of a core of expanded polystyrene (EPS) to which a 4 mm thick fiberboard panel is glued at each side. In the simulations, the fiberboard has a density $\rho = 765\ \frac{\text{kg}}{\text{m}^3}$, modulus of Elasticity $E = 3.5$ GPa, Poisson's ratio $\nu = 0.46$ and loss factor $\eta = 0.01$, while the EPS has density $\rho = 20\ \frac{\text{kg}}{\text{m}^3}$, modulus of Elasticity $E = 12$ MPa, Poisson's ratio $\nu = 0.10$ and loss factor $\eta = 0.05$.

Fig. 3 compares the hybrid TMM-SEA predictions with conventional TMM predictions and predictions using a hybrid wave-based transfer matrix method (WBTMM) model, both of which have been reported earlier [4]. The hybrid WBTMM model takes both the room and the wall modes into account, while the conventional TMM model assumes the panel to be of infinite lateral extent and the rooms to carry a diffuse field. The hybrid TMM-SEA results are also compared with measured values. All models correctly predict the resonances around 1200 Hz and around 3300 Hz, which are dilation and thickness resonance dips, respectively [4]. Below the dilation resonance frequency, the hybrid WBTMM model generally yields slightly higher transmission loss predictions than the conventional TMM model, which in its turn yields slightly higher predictions than the hybrid TMM-SEA model. Above the dilation resonance frequency, alle models predict the same transmission loss, which indicates that neither the finite size of the wall, nor individual wall resonances, nor individual room resonances influence the transmission loss at these high frequencies. The dip caused by the fundamental panel resonance, which is at

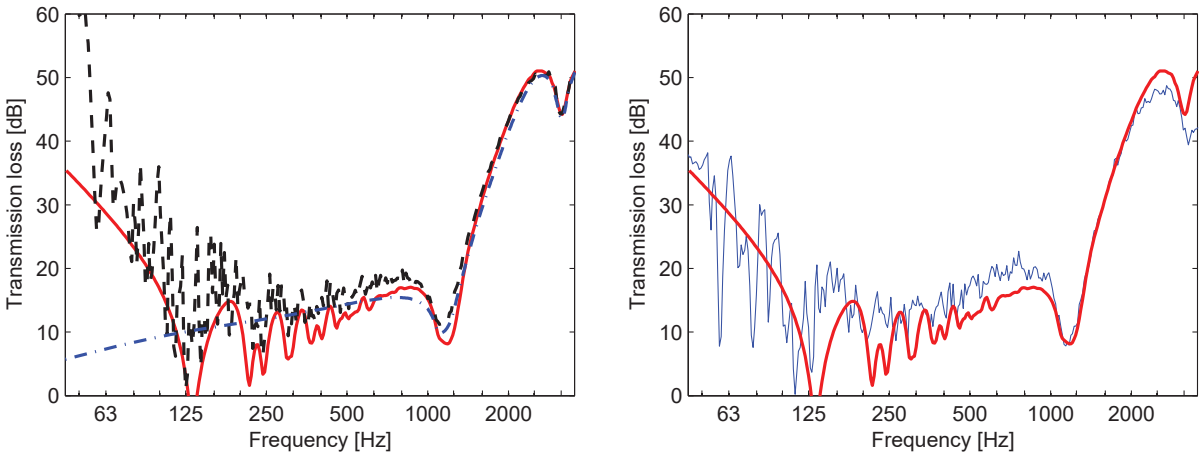

Figure 3: Sound transmission loss of a perforated brick wall as predicted with the hybrid TMM-SEA approach (red solid line), as predicted with the hybrid WBTMM approach (black dashed line), as predicted with conventional TMM (blue dash-dotted line) and as measured in the laboratory (thin blue line)

around 125 Hz, is clearly present in the hybrid TMM-SEA predictions. These predictions also agree well with the measurements, although they underestimate the transmission loss in between the first panel resonance and the dilation resonance.

7 Conclusions

A hybridization between the transfer matrix method and statistical energy analysis has been developed for computing the diffuse sound transmission through finite walls and floors that consist of layers of solid, fluid and/or poroelastic material. The approach is computationally very efficient since it obviates the numerical integration of the plane wave transmission for all possible angles of incidence, which needs to be performed in the conventional transfer matrix method. The modal behavior of the wall is approximately accounted for. The sound insulation predictions for a thin plate, a thick wall and a sandwich panel have been compared with predictions from alternative methods and with measured values, and an overall good agreement has been observed. The connection with statistical energy analysis also enables to estimate the variance of the predicted sound insulation that is inherent in the statistical diffuse field models of the rooms; this aspect will be investigated in more detail elsewhere.

REFERENCES

[1] W. Lauriks, P. Mees, and J. F. Allard. The acoustic transmission through layered systems. *Journal of Sound and Vibration*, 155(1):125–132, 1992.

[2] J.-F. Allard and N. Atalla. *Propagation of sound in porous media*. John Wiley & Sons, Chichester, UK, 2nd edition, 2009.

[3] M. Villot, C. Guigou, and L. Gagliardini. Predicting the acoustical radiation of finite size multi-layered structures by applying spatial windowing on infinite structures. *J. Sound Vib.*, 245(3):433–455, 2001.

[4] A. Dijckmans and G. Vermeir. Development of a hybrid wave based - transfer matrix model for sound transmission analysis. *Journal of the Acoustical Society of America*, 133(4):2157–2168, 2013.

[5] D. Rhazi and N. Atalla. Acoustic and vibration response of a structure with added noise control treatment under various excitations. *Journal of the Acoustical Society of America*, 135(2):693–704, 2014.

[6] P.J. Shorter and R.S. Langley. Vibro-acoustic analysis of complex systems. *Journal of Sound and Vibration*, 288(3):669–699, 2005.

[7] R.S. Langley and V. Cotoni. Response variance prediction for uncertain vibro-acoustic systems using a hybrid deterministic-statistical method. *Journal of the Acoustical Society of America*, 122(6):3445–3463, 2007.

[8] E. Reynders and R.S. Langley. Response probability distribution of built-up vibro-acoustic systems. *Journal of the Acoustical Society of America*, 131(2):1138–1149, 2012.

[9] E. Reynders, R.S. Langley, A. Dijckmans, and G. Vermeir. A hybrid finite element - statistical energy analysis approach to robust sound transmission modelling. *Journal of Sound and Vibration*, 333(19):4621–4636, 2014.

[10] L. Cremer, M. Heckl, and B.A.T. Petersson. *Structure-borne sound: Structural vibrations and sound radiation at audio frequencies*. Springer, Berlin, 3rd edition, 2005.

[11] P.J. Shorter and R.S. Langley. On the reciprocity relationship between direct field radiation and diffuse reverberant loading. *Journal of the Acoustical Society of America*, 117(1):85–95, 2005.

[12] R.S. Langley and J.A. Cordioli. Hybrid deterministic-statistic analysis of vibro-acoustic systems with domain couplings on statistical components. *Journal of Sound and Vibration*, 321(3–5):893–912, 2009.

[13] R.S. Langley. Numerical evaluation of the acoustic radiation from planar structures with general baffle conditions using wavelets. *Journal of the Acoustical Society of America*, 121(2):766–777, 2007.

[14] A. Dijckmans. *Wave based calculation methods for sound-structure interaction: application to sould insulation and sound radiation of composite walls and floors*. PhD thesis, KU Leuven, 2011.

[15] M. Schroeder. The "Schroeder frequency" revisited. *Journal of the Acoustical Society of America*, 99(5):3240–3241, 1996.

[16] G. Jacqus, S. Berger, V. Gibiat, P. Jean, M. Villot, and S. Ciukay. A homogenised vibratory model for predicting the acoustic properties of hollow brick walls. *J. Sound Vib.*, 330(14):3400–3409, 2011.